International Journal of Environmental Science and Technology (2023) 20:3861–3874
https://doi.org/10.1007/s13762-022-04245-1

ORIGINAL PAPER

A novel magnetic Fe_3O_4 carbon-shell (MFC) functionalization with lanthanum as an adsorbent for phosphate removal from aqueous solution

D. Dermawan[1,2] · V. T. Hieu[1,4] · Y.- F. Wang[1,3] · S.- J. You[1,3]

Received: 20 March 2021 / Revised: 29 September 2021 / Accepted: 20 April 2022 / Published online: 6 June 2022

Abstract

Magnetic Fe_3O_4 carbon-shell (MFC) functionalization with lanthanum (MFC@$La(OH)_3$) was successfully synthesized with various weight ratios between Fe and La utilizing the facile procedure to obtain high adsorption capacity and an easily separable adsorbent from water. FTIR result showed La-OH vibration bond and the residual NO_3^- anion confirming the La functional group's successful formation on the surface of the outer carbon shell of the magnetite core. Furthermore, the asymmetric stretch vibration of the P-O group within the HPO_4^{2-} and $H_2PO_4^-$ species of phosphate confirmed the adsorption phosphate on the surface layer of the adsorbent. The MFC@$La(OH)_3$ 1:2 has the highest BET surface area among the other adsorbents and is selected as the highest adsorbent for phosphate removal. It was discovered that the adsorption capacity increased at pH 4–6, which can be attributed to $La(OH)_3$ functional group which was protonated (positively charged), thus provoking an electrostatic interaction reaction with the negatively charged phosphate species. The equilibrium data were fit into various adsorption isotherms and found to fit well with the Freundlich model (indicating that novel adsorbent had heterogeneous surface and multilayer adsorption mechanism processes) with a maximum adsorption capacity of 30.85 mg P/g, whereas the adsorption kinetics followed pseudo-second-order kinetics. After adsorption, the magnetic separation was easily achieved, and the adsorbent could be regenerated continuously for five cycles. The current study found that the novel adsorbent has high adsorption capacity, easy to separate and recover, and appropriate for further investigation of large-scale water and wastewater treatment applications.

Keywords Phosphate · Magnetic Fe_3O_4 carbon-shell · Lanthanum · MFC@$La(OH)_3$ · Novel adsorbent · Adsorption

Introduction

Phosphorus is a mineral nutrient that is required by all living things. Both aquatic and terrestrial ecosystems require P for their growth and primary production (Hecky and Kilham 1988; Wu et al.2017a, b). Phosphate is mainly utilized for phosphate fertilizer, household detergent, and food beverages products, where possible run-off to the aquatic environment will inevitably cause several problems to both environment and living organisms. The problem can be referred to as eutrophication, which causes algae overgrowth, known as booming algae, dissolved oxygen depletion, and reduced water quality in general (Worsfold et al. 2016). There are typically three phosphate types, namely $H_2PO_4^-$, $HPO_4^{2-}$and PO_4^{3-} in an aqueous solution with a pH range of 2–10. The removal of P from water and wastewater may be done using physicochemical, biological, and combinations of both treatments to cope with such a troublesome potential occurrence

Editorial responsibility: M. Abbaspour.

✉ S.- J. You
sjyou@cycu.edu.tw

[1] Department of Environmental Engineering, College of Engineering, Chung Yuan Christian University, 200 Chung-Pei Road, Zhongli 320, Taiwan

[2] Department of Civil Engineering, Chung Yuan Christian University, Chung-Li 320, Taiwan

[3] Center for Environmental Risk Management, Chung Yuan Christian University, Chung-Li 32023, Taiwan

[4] Department of Chemistry and Environment, Vietnam-Russian Tropical Centre, Hanoi, Vietnam

(Bunce et al. 2018). Physicochemical processes of P removal are included precipitation and ion exchange mechanisms. These processes are generally reliable and effective; however, some can affect the pH of the effluent, require the addition of chemicals, and produce extraneous solids during treatment (Cornel and Schaum 2009). Biological treatment is considered a cost-effective and environmentally sustainable alternative to chemical treatment (Acevedo et al. 2012). However, the biological treatment is not wholly reliable due to fluctuating performance and difficulty in process control (Seviour et al. 2003). As a result, other methods are needed to solve the problems resulting in previous treatment methods.

Adsorption was considered the most suitable method for phosphate removal in water treatment because of convenience, ease of operation, and simplicity of design (Ahmad et al. 2012; Wang et al. 2015). Adsorption is a technique focusing primarily on surface forces of a chemical engineering unit system to perform physical or chemically binding of other substances on the unit's surface and the concentration of substances on the surface of such material. Alternatively, it can also be defined as a chemical species' partitioning between the bulk and an interface phase (Bajpai and Rajpoot 1999). In the adsorption treatment of wastewater, the adsorbent plays the most crucial part of the system.

Magnetic nano-adsorbents have advantages such as nano-size, high surface area to volume ratio, super-magnetism, large surface-bulk atom ratios, easily separated from water by an external magnetic field, abundant defect sites easy to recycle. Iron oxide for adsorbent has attracted much attention from researchers (Afkhami et al. 2010; Wang et al. 2015; Lai et al. 2016). Metal oxides with more affinity toward phosphate species at acidic pH have a more significant positive effect in removal capacity than other materials (Mitrogiannis et al. 2017; Li et al. 2019). Moreover, easy synthesis, coating, and modifying, in general, combining with its low toxicity and chemical inertness, has provided magnetic material with unparalleled versatility (Dias et al. 2011).

A fabricated nano-sized particle Fe_3O_4@mZrO_2 (Fe_3O_4 core with ZrO_2 outer shell) shows a tremendous phosphate removal capacity (up to 1.26 mmol/g). Simultaneously, it maintains more than 80% of adsorption capacity after four adsorption–desorption cycles (Sarkar et al. 2010). Moreover, the capacity for phosphate removal is also significantly affected by the pH of the solution. pH is considered the most important condition that strongly affects phosphate adsorption of the materials due to adsorption mechanisms in various pH ranges, like electrostatic binding in an acidic environment (Ahmed et al. 2019). On the other hand, under the alkaline environment, the surface of the nanomaterial is deprotonated. Thus, the binding between surface compound and phosphate is inhibited due to Donnan co-ion exclusion or electrostatic repulsion. The surface hydroxyl groups are protonated with a positive charge under low pH and attract negatively charged phosphate ions.

Lanthanum (La) has been studied progressively and proved an excellent binding chemical for phosphate. In addition, lanthanum showed superior phosphate adsorption ability (Zhang et al. 2010; Wu et al. 2017a, b; Liu et al. 2018). However, after treatment, these sorbents are difficult to isolate from wastewater. Centrifugation and filtration are two traditional methods for recovering sorbents. When separating nanoparticles from wastewater, magnetic separation is quicker and more efficient than centrifugation and filtration. However, just a few studies on the use of magnetic La-based sorbents for phosphate removal have been published due to several obstacles, such as financial problems, complicated synthetic procedures, or low phosphate removal capacity (27.8 mg P/g for Fe_3O_4@SiO_2@La_2O_3) (Lai et al. 2016).

Furthermore, the disadvantages can be overcome by combining magnetic nanoparticles (e.g., Fe_3O_4) with La to enhance removal efficiency and make sorbent separation and recovery simpler. La serves as active sites for phosphate removal in water, while the Fe_3O_4 allows for magnetic separation. In this study, Fe_3O_4 and $La(OH)_3$ were synthesized using hydrothermal and precipitation methods. The adsorption isotherm and kinetics, the adsorbent composition and dosage, the initial phosphate concentration, pH, different compete for anions, temperature, and reusability were investigated. Fourier transform infrared spectroscopy (FTIR) and Brunauer–Emmett–Teller (BET) were used to characterize the adsorbent.

Materials and methods

Materials

Iron (III) chloride hexahydrate ($FeCl_3.6H_2O$) was purchased from nacalai tesque, Japan. Lanthanum (III) nitrate hydrate ($La(NO_3)_3.xH_2O$) was purchased from Alfa Aesar, USA. Urea (CH_4N_2O) was purchased from the Japanese test, Taiwan. Glucose ($C_6H_{12}O_6$) was purchased from Sigma-Aldrich, USA. KH_2PO_4 was purchased from PanReac AppliChem, Germany. All of the chemicals used were the analytical grade reagents.

Preparation of MFC@$La(OH)_3$ adsorbent

$FeCl_3.6H_2O$ (0.006 mol), CH_4N_2O (0.1 mol), and $C_6H_{12}O_6$ (0.01 mol) were put into 40 mL of deionized water and stirred vigorously for 15 min to obtain clear yellow orange. The resulting solution was transferred into a Teflon-lined stainless-steel autoclave and heated at 180 °C for 14 h and then allowed to cool to room temperature naturally. The black precipitated magnetic microspheres were collected via

magnetic separation, followed by washing thoroughly with deionized water and absolute ethanol at least six times. The final product of MFC nanocomposites was dried overnight. The Fe_3O_4 cores were formed by reducing Fe^{3+} by glucose under alkaline conditions obtained from urea decomposition. Glucose was used to carbonize the amorphous carbon shells. The MFC nanocomposites had an average size range from 100 to 200 nm (Xuan et al. 2007).

MFC nanocomposite (0.45 g) was dispersed in 100 mL of deionized water, and then a predetermined amount of $La(NO_3)_3.xH_2O$ was injected into the suspension. Next, by adding 1 M NaOH dropwise, the pH of the combined solution was changed to 10.5. Finally, the precipitated magnetic product was collected, rinsed thoroughly with deionized water, and dried overnight (Liu et al. 2018).

Preparation of phosphate solution

Dissolving 2.2171 g of KH_2PO_4 was done to produce a 1000 mg P/L stock (dried in 105 °C for 1 h beforehand) in 500 mL deionized water. This recipe follows the instruction from EPA, Taiwan. All phosphate in this study refers to orthophosphate unless otherwise specified.

Adsorption isotherm studies

The adsorption isotherm is used to define the characteristics of the adsorption process between liquid and solid phases when it reaches equilibrium, and an adsorption isotherm study was conducted. The Langmuir and Freundlich models were chosen to fit the equilibrium data obtained from the batch adsorption experiments by varying the initial concentration of phosphate. The adsorption isotherm experiment was conducted by introducing 0.5 g/L of adsorbents to a 50 mL solution with various initial phosphate concentrations (1, 5, 10, 15, and 20 mg/L)m and they were placed onto an orbital shaker at 150–200 rpm for 24 h for absolute equilibrium. After that, the supernatant was taken out and filtered, and then the phosphate residue was measured. The experimental analysis results are the mean values of the triplicated experiments of the phosphate adsorption process. The amount of equilibrium adsorption (q, mg/g) for phosphate was determined following Eq. (1).

$$q_e = \frac{(C_0 - Ce)V}{m} \tag{1}$$

where C_0 = initial concentration of adoptive (mg/L); Ce = concentration of adoptive at the time t (mg/L); V = volume of bulk solution (L); m = mass of adsorbent.

The Langmuir isotherm is based on the assumption that the adsorbent surface contains homogeneous binding sites with identical sorption energies and no interaction with the adsorbed molecules. The Langmuir isotherm model was adopted to analyze the isotherm data and expressed according to Eq. (2) (Freundlich 1906; Wu et al. 2017a, b; Li et al. 2019).

$$\frac{C_e}{q_e} = \frac{1}{q_{max}k_L} + \frac{1}{q_{max}}C_e \tag{2}$$

where K_L is the Langmuir equilibrium constant (L/mg) and q_{max} is the monolayer adsorption capacity (mg/g). This equation is usually evaluated by a separate factor, R_L, which can be calculated according to Eq. (3).

$$R_L = \frac{1}{1 + k_L C_0} \tag{3}$$

where C_0 is the maximum initial concentration of solute (mg/L) and this element demonstrates the nature of the adsorption process and the isotherm as follows: unfavorable ($R_L > 0$), linear ($R_L = 0$), favorable ($0 < R_L < 1$), and irreversible ($R_L = 0$).

The Freundlich isotherm is one of the earliest models that explain non-ideal and irreversible adsorption without limiting monolayer formation, so multilayer and non-uniform distribution adsorption heat and heterogeneous surface affinities can be added to this empirical model according to Eq. (4) (Freundlich 1906; Wu et al. 2017a, b; Li et al. 2019).

$$\log q_e = \log k_f + \frac{1}{n}\log C_e \tag{4}$$

Adsorption kinetic studies

The experimental data at different contact times corresponding to changes in the amount of phosphate adsorbed to assess the kinetic adsorption of phosphate onto the adsorbents were fitted into three other kinetic models, including pseudo-first-order, pseudo-second-order, and intra-particle diffusion. The adsorption kinetics was carried out by applying 0.5 g/L of adsorbent material with a phosphate concentration of 5 mg/L to a 50 mL solution and placed firmly on an orbital shaker at 150–200 rpm. To be precise, at each time interval, 30th, 60th, 120th, 240th, 360th, 480th, and 600th minutes 1 mL of supernatant was taken out and filtered. Phosphate residue was measured. The experimental analysis results are the mean values of the triplicated experiments of the phosphate adsorption process. The pseudo-first-order model (Eq. (5)) (Lagergren 1898), the pseudo-second-order model (Eq. (6)) (Ho and McKay 1999), and the intra-particle diffusion model (Eq. (7)) (Weber 1963) were adopted and expressed as the following equations in order to analyze the kinetic data:

$$\log(q_e - q_t) = \log q_e - \frac{k_{pL}}{t}t \tag{5}$$

where q_e = adsorption capacities at equilibrium (mg/g); q_t = adsorption capacities at time t (mg/g); k_{pL} = pseudo-first-order rate constant (min^{-1}).

$$\frac{t}{q} = \frac{1}{k_2 q_e^2} + \frac{t}{q_e} \tag{6}$$

The pseudo-second-order rate constant is k_2 (g/mg min), and the other symbols have the same meaning as describe in the above equation. A plot of $\frac{t}{q}$ versus t gives a linear line for this order-compliant kinetics. The slope from the given linear equation is $\frac{1}{q_e}$, and the intercept is $\frac{1}{k_2 q_e^2}$.

$$q_t = k_{int} t^{1/2} + B \tag{7}$$

The intra-particle diffusion rate constant is k_{int} (mg/g $min^{0.5}$) and B is the initial adsorption (mg/g). A plot of q_t and $t^{1/2}$ gives a linear line to an adsorption process that is compliant with it, which its slope is k_{int}.

Effect of the adsorbent dosage and pH

In order to investigate the suitable dosage of adsorbent, different amounts of adsorbent (0.5, 0.75, 1, and 1.5 g/L) were introduced to 50 mL solution containing 5 mg/L of phosphate with the reaction time of 24 h for equilibrium. The residue of phosphate was filtered and measured.

In a similar procedure, the adsorbent value of 0.05 g was applied to 50 mL of 5 mg P/L solution with different initial pH using NaOH and H_2SO_4 solution to achieve a pH value ranging from 2 to 12 to investigate the effect of pH toward phosphate removal efficiency.

Effect of different compete anions

The effect of different compete for anions on the amount of phosphate adsorbed was investigated by adding 5 mg P/L in 50 mL solution, and another 5 mg/L of Cl^-, SO_4^{2-} and HCO_3 in the form of sodium salt was added to the phosphate solution in a separate container. The combined solution was placed on an orbital shaker at 190 rpm for 24 h to ensure its equilibrium. Then residue phosphate concentration was measured to evaluate MFC@$La(OH)_3$ adsorbent's affinity toward phosphate.

Effect of temperature

The effect of different temperatures on its adsorption behavior was carried out. In this experiment, 23 and 37 °C are two temperature parameters chosen for these studies. Langmuir and Freundlich models were also applied for these studies to check for any alternation to its actual result, which was carried out at typical room temperature.

The reusability of MFC@$La(OH)_3$ adsorbent

The reusability test was carried out by applying 0.025 g of adsorbent to 50 mL of 1 mg P/L solution at room temperature for 1 h, followed by the desorption process using 50 mL 1 M NaOH for 2 h. The residue of phosphate concentration from each cycle was measured to determine the adsorbent's removal efficiency after continuous recycling.

Adsorbent characterization

The Brunauer–Emmett–Teller (BET) method was used to measure the specific surface areas via N_2 adsorption studies on TriStar 3000 V6.07 A. In addition, the Fourier transform infrared (FTIR) spectrometer (Jasco FT/IR-6500) was used to analyze the surface functional groups' composition and structure. The result will be depicted in wavenumber ranging from 400 to 2000 cm^{-1}.

Phosphate measurement

After each batch study test, the residue of phosphate concentration was measured via the UV–Vis spectrophotometer Genesys™ 10S (Thermo Scientific, USA) at a wavelength equal to 880 nm. The method used in this research is the ascorbic blue method.

Results and discussion

Adsorption isotherm

In order to understand the adsorption process, adsorption isotherm models are used. Langmuir and Freundlich isotherm models were used to analyze the adsorption equilibrium experimental data obtained for phosphate adsorption. Figures 1 and 2 present the plots of Langmuir and Freundlich isotherm models for phosphate adsorption onto MFC@$La(OH)_3$. The correlation coefficient (R^2) values are presented in Table 1, and the adsorption process of phosphate onto the adsorbent was found to follow the Freundlich isotherm model. All of the adsorbents were well suited with the Freundlich model, which indicated that MFC@$La(OH)_3$ had heterogeneous surface and multilayer adsorption mechanism processes (Wu et al. 2017a, b). In the Freundlich model, *n* is a factor to explain the mechanism of adsorption. The value of n was between 1 and 10 in this research, indicating that the adsorption of phosphate anions on the adsorbent surface was favorable (Ahmed et al. 2017). The Freundlich maximum adsorption capacity was 30.85 mg P/g. The adsorption capacity of the

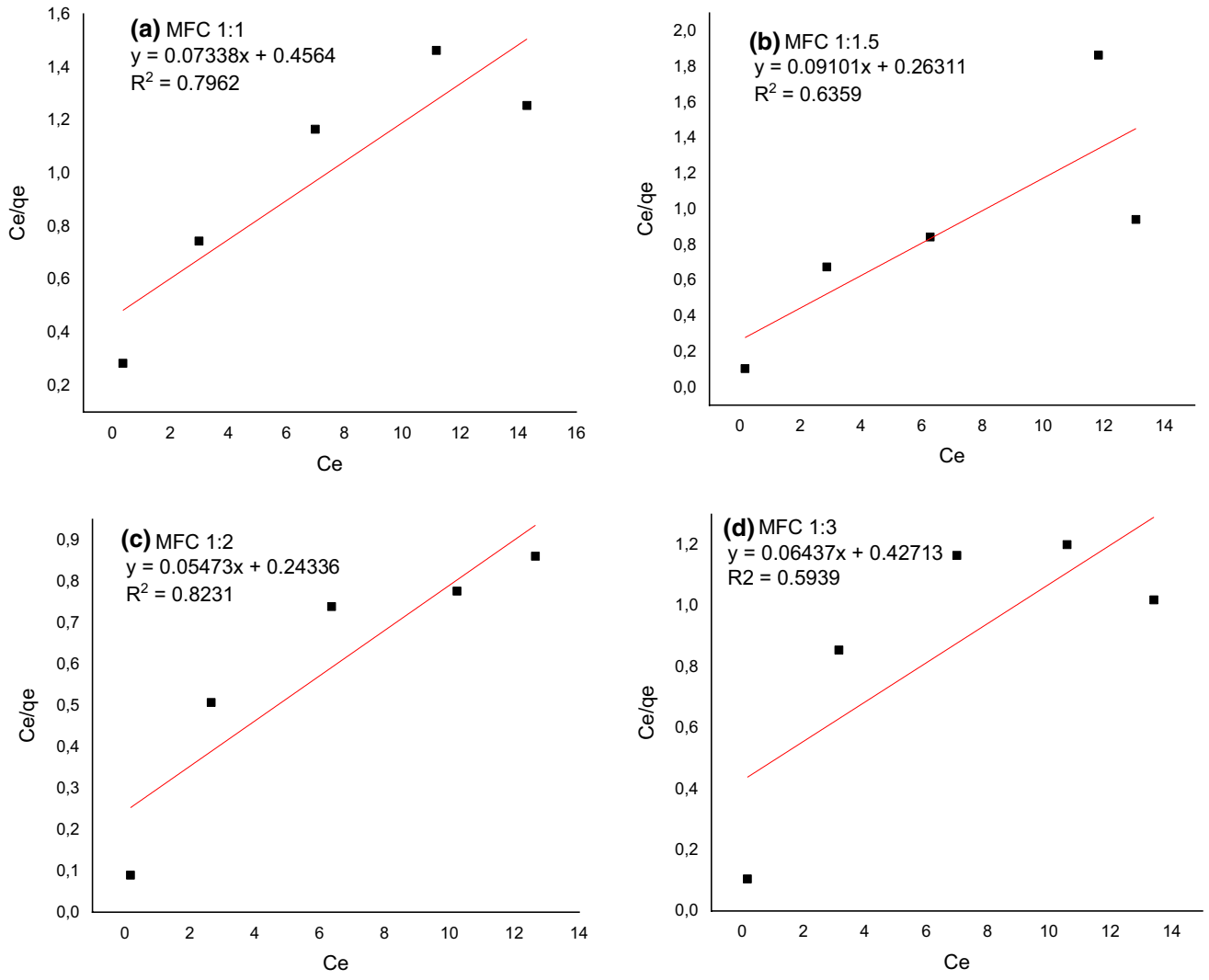

Fig. 1 Langmuir isotherm models for the adsorption of phosphate onto MFC@La(OH)$_3$ of **a** MFC 1:1, **b** MFC 1:1.5, **c** MFC 1:2, **d** MFC 1:3

novel adsorbent compared with other research is presented in Table 2.

Adsorption kinetic

Adsorption kinetics models were used to understand adsorption pathways. Three different kinetic models were used to fit the experimental data: the pseudo-first-order, pseudo-second-order, and intra-particle diffusion models. Figures 3, 4, 5 and Table 3 denote that MFC@La(OH)$_3$ complied greatly with the pseudo-second-order kinetic model ($R^2 = 0.99$) than the pseudo-first-order kinetic model ($R^2 > 0.4$) or intra-particle diffusion ($R^2 > 0.55$). Theoretically, the pseudo-second-order model assumes that the adsorption rate of phosphate uptake is proportional to the square of the difference between the amount of phosphate absorbed with time and phosphate absorbed at equilibrium. The pseudo-second-order kinetic implies phosphate's adsorption on the novel adsorbent mixed physical and chemical adsorption (Ahmed et al. 2017; Li et al. 2019).

Effect of MFC@La(OH)$_3$ adsorbent composition

The effect of MFC@La(OH)$_3$ adsorbent composition from 1:1, 1:1.5, 1:2, and 1:3 were investigated. The results are presented in Fig. 6. MFC@La(OH)$_3$ 1:2 denoted superior removal capacity to other compositions with more than 50% efficiency, while the second-highest, MFC@La(OH)$_3$ 1:1.5 could effectively remove nearly 40% of phosphate in the solution. Moreover, all the adsorbent compositions adsorbed phosphate in a considerable fast peace, at around 30 min after contact, followed by a stable adsorb rate throughout the length of the experiment and gradually reached its maximum capacity.

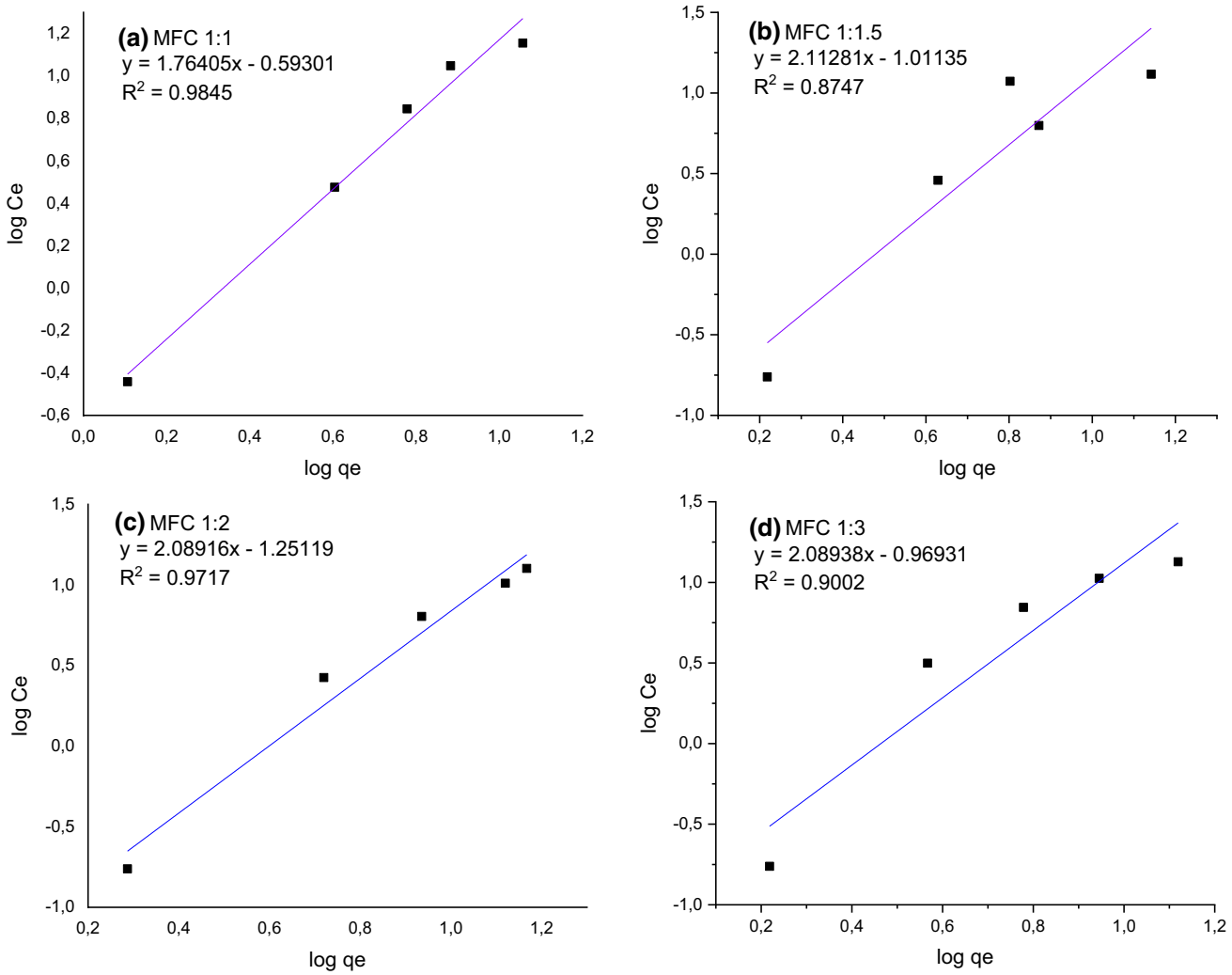

Fig. 2 Freundlich isotherm models for the adsorption of phosphate onto MFC@La(OH)$_3$ of **a** MFC 1:1, **b** MFC 1:1.5, **c** MFC 1:2, **d** MFC 1:3

Table 1 Langmuir and Freundlich isotherm models for the adsorption of phosphate on MFC@La(OH)$_3$

Adsorbents composition	Langmuir				Freundlich		
	Qm (mg/g)	K_L (L/mg)	R_L	R^2	1/n	K_f (L/g)	R^2
MFC@La(OH)$_3$ 1:1	13.62	0.16	0.24	0.514	0.56	2.20	0.979
MFC@La(OH)$_3$ 1:1.5	10.99	0.35	0.13	0.728	0.41	3.24	0.866
MFC@La(OH)$_3$ 1:2	18.28	0.22	0.18	0.060	0.47	4.04	0.833
MFC@La(OH)$_3$ 1:3	15.53	0.15	0.25	0.458	0.43	3.09	0.962

In the first 30 min, all compositions denoted a rapid adsorption process due to the physical sorption. The adsorption of adsorbent toward phosphate was either fast migration to the adsorbent's external surface and surface charge interaction. In addition, iron and lanthanum attract negatively charged phosphate as an active phosphate-binding site (Ahmed et al. 2019). Finally, the adsorption process reached an equilibrium stage over the adsorbent's small pores' diffusion and the adsorbate's chemical binding reaction (Li et al. 2019).

Effect of the initial concentration of phosphate

The effect of the initial concentration of phosphate from 1, 5, 10, 15 to 20 mg/L was investigated. The results are presented in Fig. 7. The MFC@La(OH)$_3$ 1:2 adsorbent composition

Table 2 The adsorption capacity of adsorbents compared with other research

Type of adsorbent	Dosage (g/L)	Phosphate concentration (mg P/L)	Efficiency (%)	Adsorption capacity (mg P/g)	References
Fe_3O_4@Sio_2 @La_2O_3	1	2	95	27.8	Lai et al. (2016)
La-SBA-15	1	50	95	24.6	Yang et al. (2011)
Phoslock	0.92	1	n/a	10.5	Haghseresht et al. (2009)
NT-25La (La-modified Bentonite)	0.375	5	90	14	Kuroki et al. (2014)
MFC@$La(OH)_3$	0.5	5	54	30.85	This study

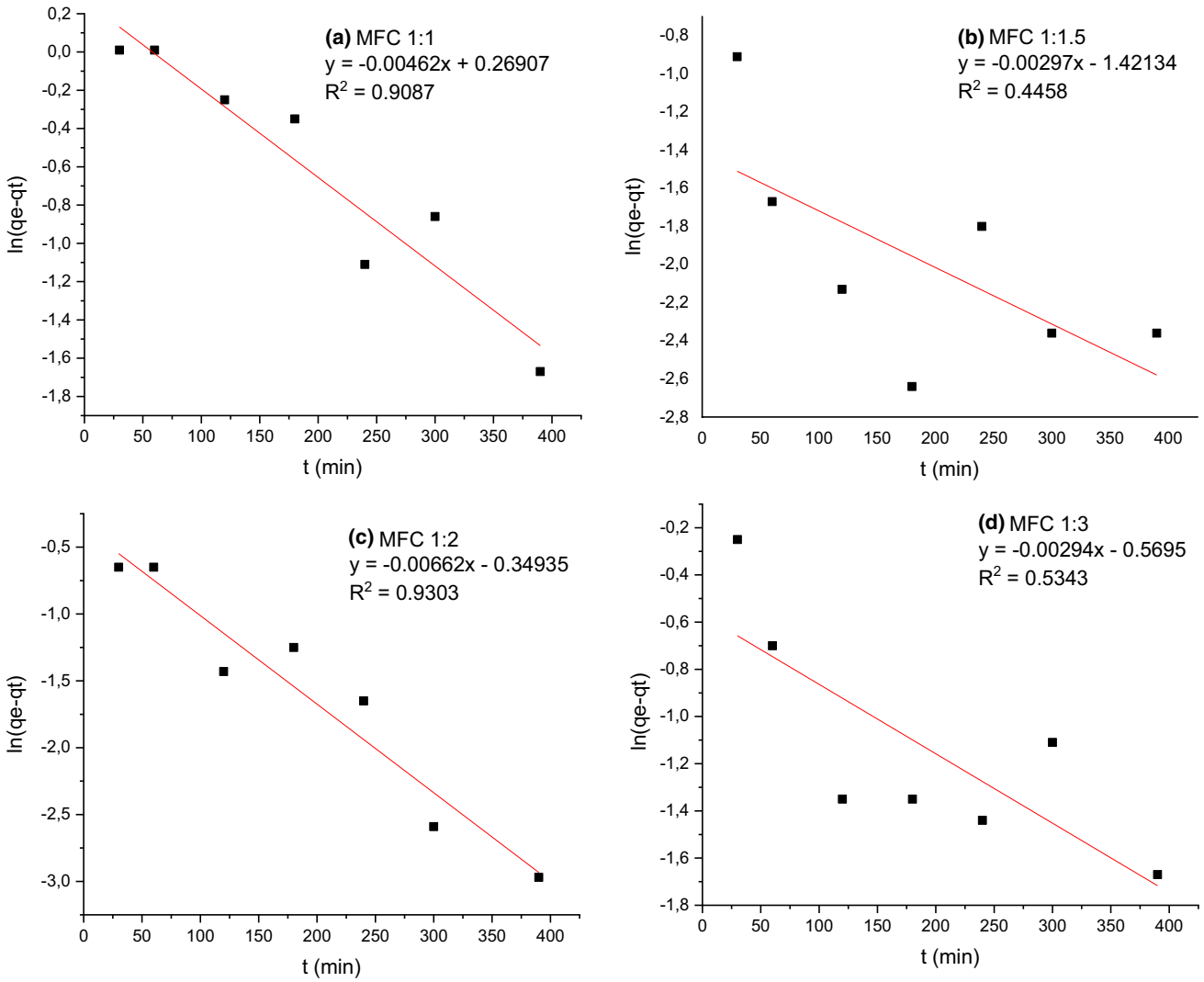

Fig. 3 Pseudo-first-order kinetic models for the adsorption of phosphate onto MFC@$La(OH)_3$ of **a** MFC 1:1, **b** MFC 1:1.5, **c** MFC 1:2, **d** MFC 1:3

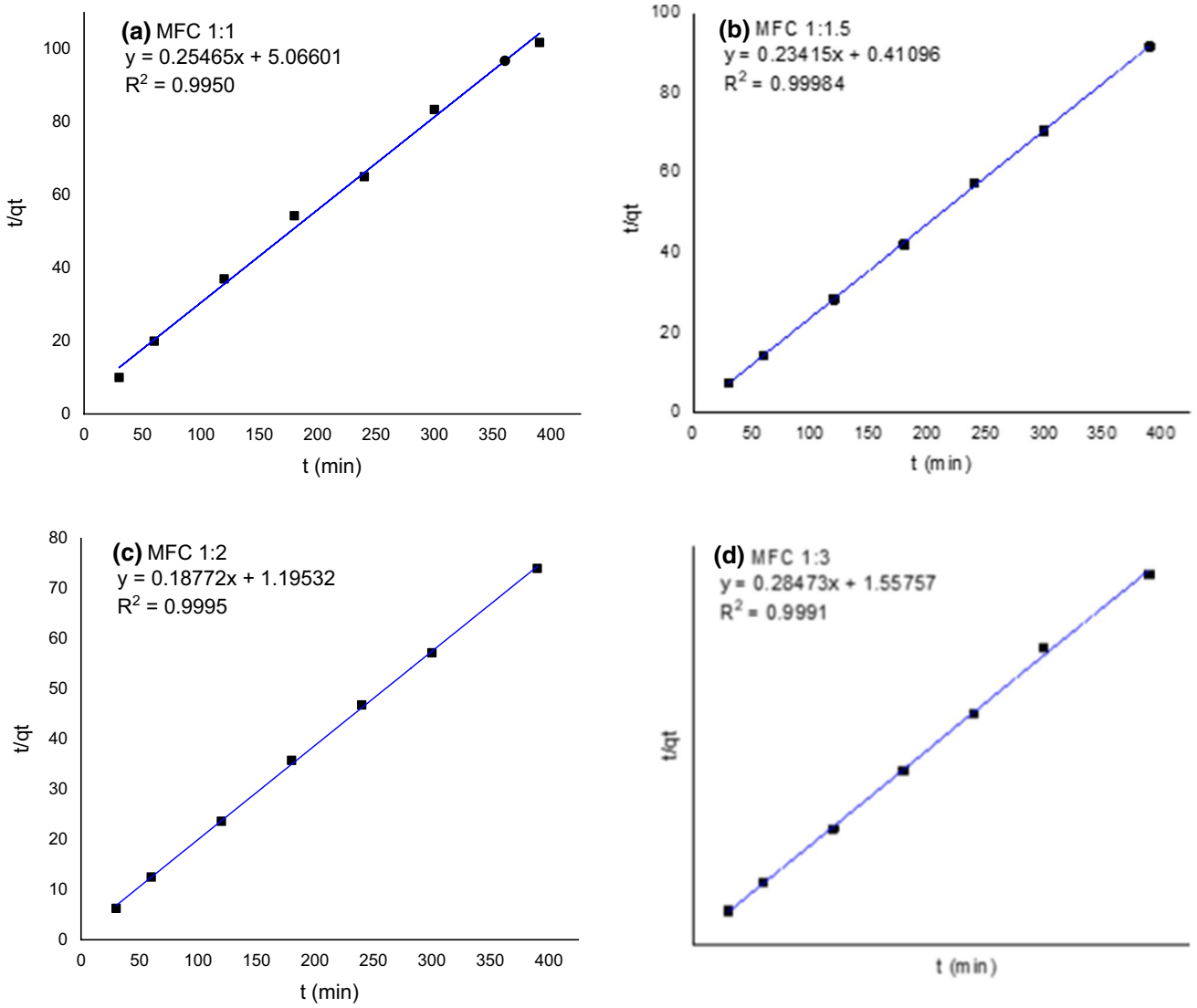

Fig. 4 Pseudo-second-order kinetic model for the adsorption of phosphate onto MFC@La(OH)$_3$ of **a** MFC 1:1, **b** MFC 1:1.5, **c** MFC 1:2, **d** MFC 1:3

performed well when applied to 1 mg P/L solution, with up to a near-complete phosphate removal of 100% MFC@La(OH)$_3$ 1:1.5 and 1:3 could remove around 80% of phosphate. However, there was a decrease in all material, nearly twofold, when introduced to a 5 mg P/L solution. As a result, the efficiency of MFC@La(OH)$_3$ 1:2 dropped to around 54% removal efficiency, which was significantly higher than the other ratio. This trend was identical throughout all other phosphate concentrations, proving the ratio between Fe and La of 1:2 was the most suitable ratio during the synthesis procedure. This adsorbent is effective in removing low-concentration phosphate in water bodies.

Effect of the adsorbent dosage

The effect of adsorbent dosage on phosphate adsorption was investigated. The effect of adsorbent dosage during the adsorption process is denoted in Fig. 8. It depicted that the amount of phosphate adsorbed onto adsorbent increases with increasing adsorbent dosage. The amount, pore volume, and pore size of adsorbents highly influence the adsorption rate, and phosphate adsorbed onto the adsorbent surface. The first dosage of adsorbent, 0.5 g/L, reached a removal of nearly 53%. A dosage of 1 and 1.5 g/L expressed its superior performance within the same condition, with a maximum of nearly 70 and 89% phosphate being removed, respectively.

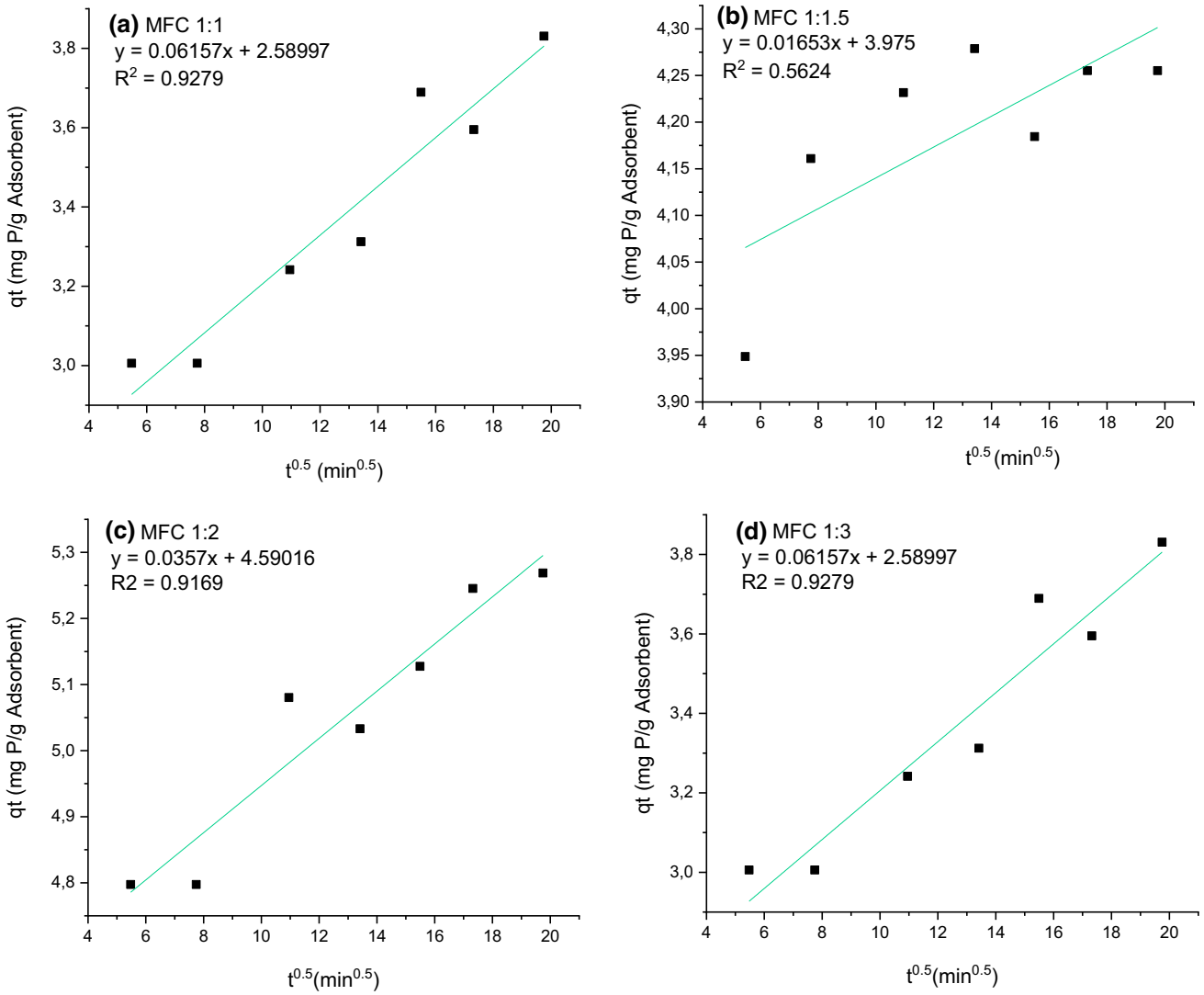

Fig. 5 Intra-particle diffusion models for the adsorption of phosphate onto MFC@$La(OH)_3$ of **a** MFC 1:1, **b** MFC 1:1.5, **c** MFC 1:2, **d** MFC 1:3

Table 3 Kinetic model parameters for the adsorption of phosphate on MFC@$La(OH)_3$

Model	Parameter	Unit	MFC@$La(OH)_3$ 1:1	MFC@ $La(OH)_3$ 1:1.5	MFC@ $La(OH)_3$ 1:2	MFC@ $La(OH)_3$ 1:3
Pseudo-first-order kinetic	q_e	mg/g	5.382	5.809	5.021	5.843
	K	min^{-1}	−0.272	1.424	0.347	0.571
	R^2		0.890	0.334	0.916	0.534
Pseudo-second-order kinetic	q_e	mg/g	3.926	4.272	5.328	5.328
	K	g/mg min	0.013	0.133	0.029	0.029
	R^2		0.994	0.999	0.999	0.998
Intra-particle diffusion	K	mg/g $min^{0.5}$	0.0616	0.0165	0.0357	0.0332
	B	mg/g	2.590	3.975	4.5902	2.8975
	R^2		0.913	0.474	0.900	0.611

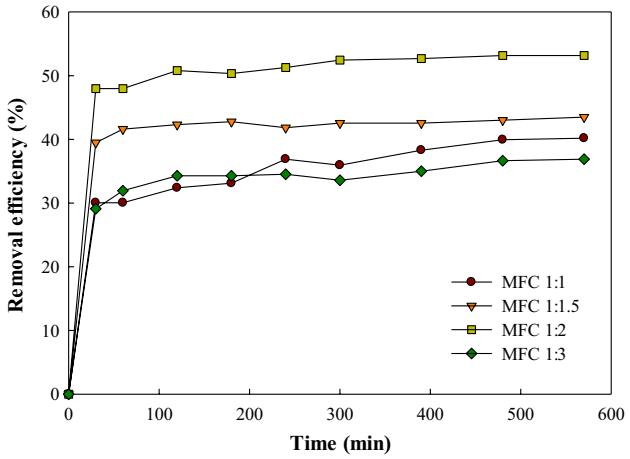

Fig. 6 Effect of contact time and MFC@$La(OH)_3$ composition on the adsorption of phosphate

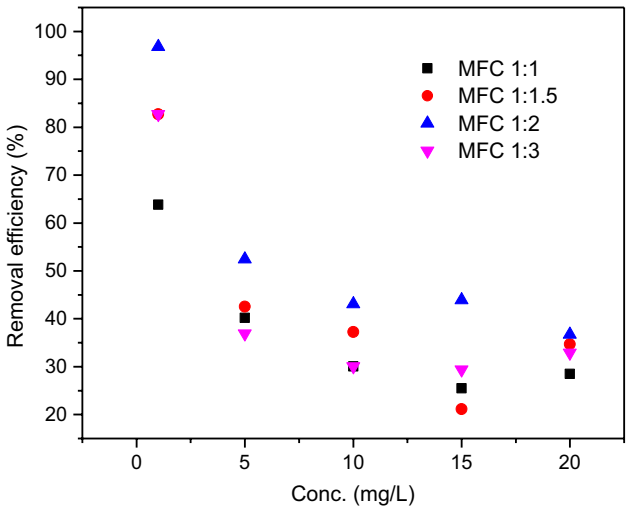

Fig. 7 Effect of initial phosphate concentration on the adsorption of phosphate onto MFC@$La(OH)_3$

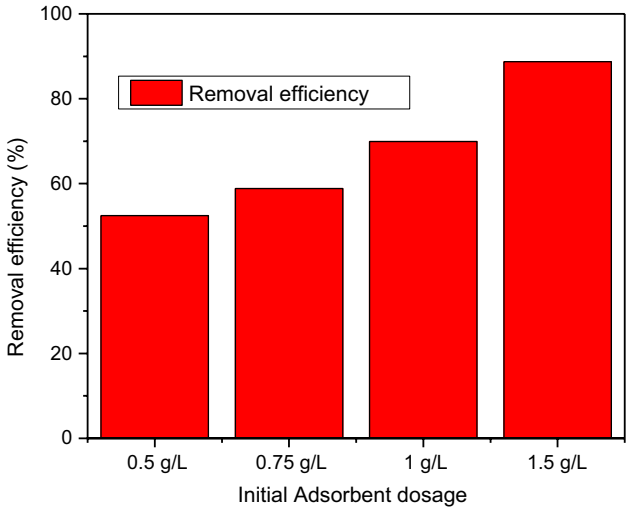

Fig. 8 Effect of MFC@$La(OH)_3$ dosage on the adsorption of phosphate

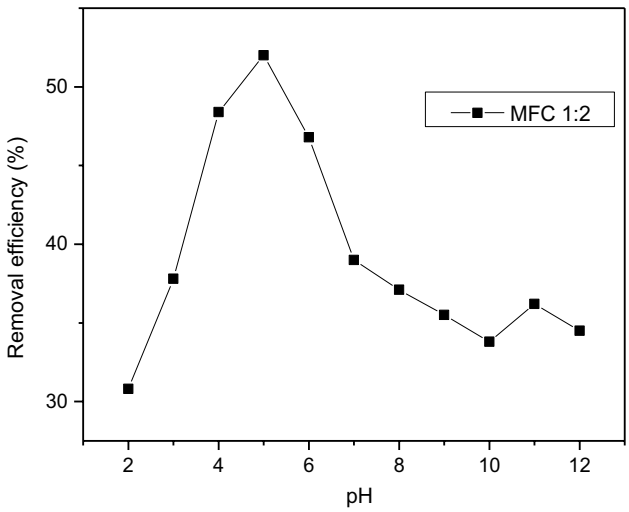

Fig. 9 Effect of pH on the adsorption of phosphate onto MFC@$La(OH)_3$

Effect of pH

The effect of pH on phosphate adsorption was investigated. Figure 9 depicts that the removal of MFC@$La(OH)_3$ 1:2 is significantly affected by the pH. With a high pH range, adsorb phosphate's ability was severely inhibited, drop significantly from above 50% to around 30%. The explanation for this phenomenon was that the $La(OH)_3$ functional group was deprotonated (anionic). As a result, it became negatively charged, thus provoking an electrostatic repulsive reaction with the also negatively charged monovalent $H_2PO_4^-$, the main phosphate species in this pH range (Liu and Zhang 2015; Wu et al. 2017a, b; Liu et al. 2018). This result firmly concluded that MFC@$La(OH)_3$ 1:2 was a greatly pH-dependent material.

Effect of different compete for anions

In a real application, such as domestic or industrial wastewater, phosphate usually co-exists with numerous anions and cations. Therefore, the effect of competing anions like chloride, sulfate, and bicarbonate on the adsorption process was investigated. The results are depicted in Fig. 10. The MFC@$La(OH)_3$ 1:1.5 and MFC@$La(OH)_3$ 1:2 adsorbents had slight interference. However, each test's differences were negligible, only around 3–5%, apart from the control test result at around 53%.

In conclusion, the effect of different competitive anions in the same solution did not impact the adsorbent's phosphate

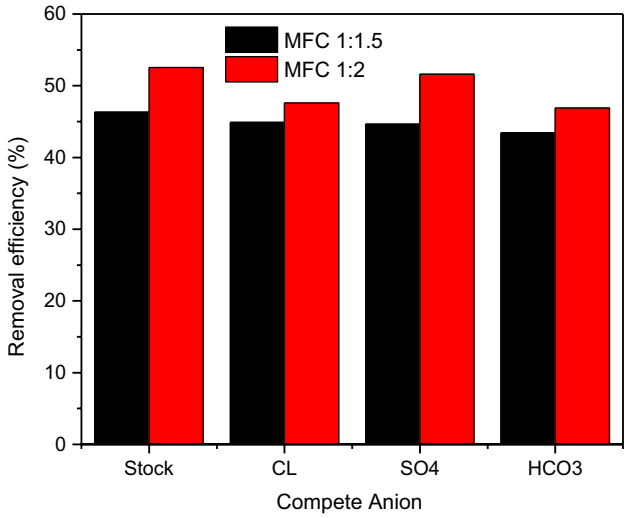

Fig. 10 Effect of different compete for anions on the adsorption of phosphate onto MFC@La(OH)$_3$

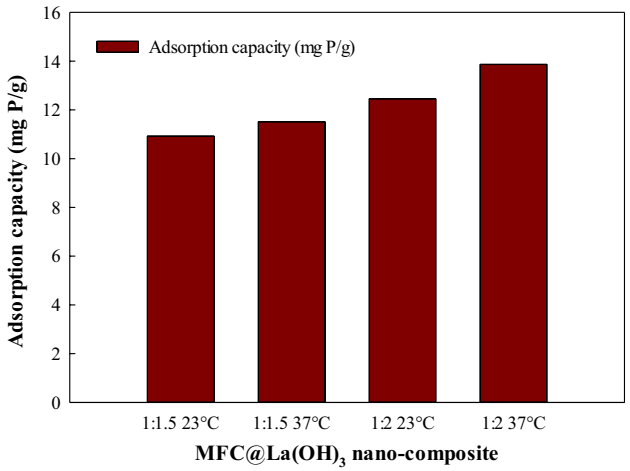

Fig. 11 Effect of temperatures on the adsorption of phosphate onto MFC@La(OH)$_3$

adsorption. This test pointed out that the material had an excellent phosphate affinity to other anions, thus proved a great candidate for any phosphate scenarios, either domestically or industrially, and recovery or removal.

Effect of temperature

The adsorption capacities at two temperatures were determined to analyze the effect of temperature on the adsorption process. Temperatures of 23 °C represented room temperature. A temperature of 37 °C was chosen because it might still be economically feasible for the actual application of the adsorbent at a higher temperature. Figure 11 and Table 4 denote that the adsorption was facilitated at higher temperatures. The rate constant (K_f) of MFC@La(OH)$_3$ 1:2 and MFC@La(OH)$_3$ 1:1.5 had increased from 2.2 to 3.77 and from 3.24 to a staggering 5.71, respectively. This feature had concluded that the novel adsorbent had an endothermic process, which contributed to the increase in the adsorption capability by increasing the adsorption temperature (Wu et al. 2014).

The reusability of MFC@La(OH)$_3$ adsorbent

Five continuous adsorption and desorption cycles were performed to evaluate the reusability MFC@La(OH)$_3$ 1:1.5 and 1:2 adsorbent. Figure 12 points out that adsorbent expressed a gradual but slow decline in phosphate removal efficiency, with nearly 5% loss for each cycle. This result had denoted that practical application for continuous use and reuse was highly possible due to facile and economical synthesis procedures and a slow decline in its removal capacity.

Characterization of MFC@La(OH)$_3$ adsorbent

MFC@La(OH)$_3$ 1:2 adsorbent as the best composition was characterized using FTIR and BET techniques. The FTIR result of MFC@La(OH)$_3$ 1:2 is presented in Fig. 13. A new I.R. bond at 573 cm^{-1} could be observed in the MFC loaded with La(OH)$_3$, which was the characteristic of La-OH vibration bond. Moreover, a new peak of the MFC@La(OH)$_3$ 1:2 at 1381 cm^{-1} represented the residual NO_3^- anion. These additional peaks confirmed the Lanthanum functional group's successful formation on the surface of the outer carbon shell of the magnetite core.

Furthermore, a new I.R. bond of 1043 cm^{-1} represented the asymmetric stretch vibration of the P-O group within the HPO_4^{2-} and $H_2PO_4^-$ species of phosphate confirmed the adsorption phosphate on the surface layer of the adsorbent.

Table 4 Adsorption isotherm model parameters for the adsorption of phosphate on MFC@La(OH)$_3$

Adsorbent composition	Langmuir				Freundlich		
	Qm	K_L	R_L	R^2	1/n	K_f	R^2
MFC@La(OH)$_3$ 1:1.5@23 °C	13.28	0.192	0.2	58.85	0.56	2.20	98.45
MFC@La(OH)$_3$ 1:1.5@37 °C	18.15	0.17	0.23	65.22	0.43	3.77	91.4
MFC@La(OH)$_3$ 1:2@23 °C	14.04	0.22	0.18	76.24	0.41	3.24	87.48
MFC@La(OH)$_3$ 1:2@37 °C	15.50	0.34	0.13	80.84	0.29	5.71	93.74

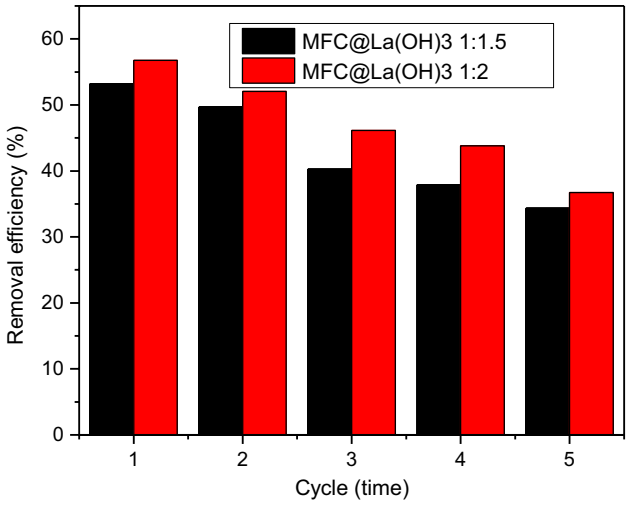

Fig. 12 Reusability of MFC@La(OH)$_3$ in continuous tests

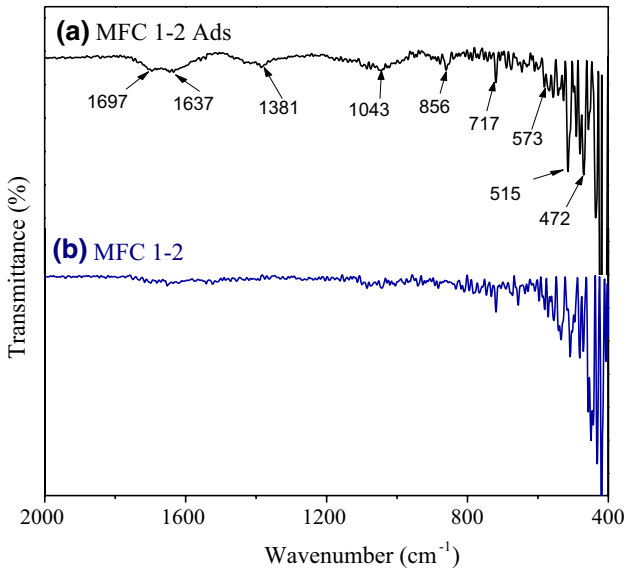

Fig. 13 FTIR spectra of MFC@La(OH)$_3$ 1:2 **a** after phosphate adsorption and **b** before phosphate adsorption

Table 5 BET surface area, pore size, and pore volume of the novel adsorbents

Adsorbents composition	BET surface area (m^2/g)	Pore size (nm)	Pore volume (cm^3/g)
MFC@La(OH)$_3$ 1:1.5	8.3350	11.6767	0.0252
MFC@La(OH)$_3$ 1:2	18.8145	14.1676	0.0689
MFC@La(OH)$_3$ 1:3	11.1232	13.8887	0.0399

Moreover, HPO_4^{2-} and $H_2PO_4^-$ phosphate species were expected in the research's pH range, providing valuable information for the phosphate removal potential of the MFC@La(OH)$_3$ adsorbent.

The surface area and pore size distributions of MFC@La(OH)3 1:1.5, MFC@La(OH)$_3$ 1:2 and MFC@La(OH)$_3$ 1:3 were characterized using BET (Brunauer–Emmett–Teller) and BJH (Barrett–Joiner–Helenda) pore size distribution methods, shown in Table 5. The MFC@La(OH)$_3$ 1:2 has the highest BET surface area among the other nanocomposites and is selected as the highest adsorbent for phosphate removal experiments. Table 5 denotes the BET, pore size, and pore volume results among the nanocomposite adsorbents.

Conclusion

The adsorbent had been successfully synthesized through two stages of the quick and facile procedure. The adsorption data were well suited with the Freundlich model, and the adsorption behavior complied greatly with the pseudo-second-order kinetic model. It had a high adsorption capacity of 30.85 mg P/g. MFC@La(OH)$_3$ 1:2 ensured superior removal capacity to others with more than 50% efficiency. Moreover, its kinetic behavior depended on pH, where the performance was excellent at a pH range from 4 to 6. Different competing anions in the same solution did not carry much impact on phosphate adsorption. In addition, the novel adsorbent had an endothermic process. Finally, it could be used and regenerated continuously for at least five cycles while retains its acceptable removal efficiency higher. Thus, the novel adsorbent has high adsorption capacity, easy to separate and recover, and promising to be applied in the water and wastewater field.

Acknowledgements This paper and the research would not have been possible without support from the Circular Society Laboratory and Center for Environmental Risk Management, Environmental Engineering Department, Chung Yuan Christian University.

Author contributions DD was involved in method investigation, writing, editing, and review. VTH was involved in method investigation, data investigation, and writing. YF Wang was involved in method investigation, supervision, and review. SJ You was involved in conceptualization, method investigation, supervision, and review.

Funding This research was supported by the Centre of Environmental Risk Management, Chung Yuan Christian University (Project No: 109609432).

Declarations

Conflict of interest The authors declare that they have no known competing financial interests or personal relationships that could have appeared to influence the work reported in this paper.

References

Acevedo B et al (2012) Metabolic shift of polyphosphate-accumulating organisms with different levels of polyphosphate storage. Water Res 46(6):1889–1900. https://doi.org/10.1016/j.watres.2012.01.003

Afkhami A, Saber-Tehrani M, Bagheri H (2010) Modified maghemite nanoparticles as an efficient adsorbent for removing some cationic dyes from aqueous solution. Desalin 263(1–3):240–248. https://doi.org/10.1016/j.desal.2010.06.065

Ahmad T et al (2012) The use of date palm as a potential adsorbent for wastewater treatment: a review. Environ Sci Pollut Res 19(5):1464–1484. https://doi.org/10.1007/s11356-011-0709-8

Ahmed S et al (2017) Hexamethylene tetramine-assisted hydrothermal synthesis of porous magnesium oxide for high-efficiency removal of phosphate in aqueous solution. J Environ Chem Eng 5(5):4649–4655. https://doi.org/10.1016/j.jece.2017.09.006

Ahmed S et al (2019) Recent progress on adsorption materials for phosphate removal. Recent Pat Nanotech. https://doi.org/10.2174/1872210513666190306155245

Bajpai AK, Rajpoot M (1999) Adsorption techniques. J Sci Ind Res 58:844–860

Bunce JT et al (2018) A review of phosphorus removal technologies and their applicability to small-scale domestic wastewater treatment systems. Front Environ Sci. https://doi.org/10.3389/fenvs.2018.00008

Cornel P, Schaum C (2009) Phosphorus recovery from wastewater: needs, technologies and costs. Water Sci Technol 59(6):1069–1076. https://doi.org/10.2166/wst.2009.045

Dias AMGC et al (2011) A biotechnological perspective on the application of iron oxide magnetic colloids modified with polysaccharides. Biotech Adv 29(1):142–155. https://doi.org/10.1016/j.biotechadv.2010.10.003

Freundlich HMF (1906) Uber die adsorption in losungen. Z Phys Chem. https://doi.org/10.1515/zpch-1907-5723

Haghseresht F, Wang S, Do DD (2009) Applied clay science a novel lanthanum-modified bentonite, phoslock, for phosphate removal from wastewaters. Appl Clay Sci 46(4):369–375. https://doi.org/10.1016/j.clay.2009.09.009

Hecky RE, Kilham P (1988) Nutrient limitation of phytoplankton in freshwater and marine environments: a review of recent evidence on the effects of enrichment. Limnol Oceanogr. https://doi.org/10.4319/lo.1988.33.4part2.0796

Ho YS, McKay G (1999) Pseudo-second order model for sorption processes. Pro Biochem. https://doi.org/10.1016/S0032-9592(98)00112-5

Kuroki V et al (2014) Use of a La (III) -modified bentonite for effective phosphate removal from aqueous media. J Hazard Mater 274:124–131. https://doi.org/10.1016/j.jhazmat.2014.03.023

Lagergren S (1898) About the theory of so-called adsorption of solid substance. Handlinger. https://doi.org/10.4236/ss.2014.52008

Lai L et al (2016) Adsorption of phosphate from water by easily separable Fe_3O_4 @ SiO_2 core/shell magnetic nanoparticles functionalized with hydrous lanthanum oxide. J Colloid Interf Sci 465:76–82. https://doi.org/10.1016/j.jcis.2015.11.043

Li T et al (2019) Magnetic polymer-supported adsorbent with two functional adsorption sites for phosphate removal. Environ Sci Pollut Res 26(32):33269–33280. https://doi.org/10.1007/s11356-019-06351-z

Liu X, Zhang L (2015) Removal of phosphate anions using the modified chitosan beads: adsorption kinetic, isotherm and mechanism studies. Powder Tech 277:112–119. https://doi.org/10.1016/j.powtec.2015.02.055

Liu T et al (2018) Highly effective wastewater phosphorus removal by phosphorus accumulating organism combined with magnetic sorbent MFC @ La(OH)3. Chem Eng J 335:443–449. https://doi.org/10.1016/j.cej.2017.10.117

Mitrogiannis D et al (2017) Removal of Phosphate from aqueous solutions by adsorption onto $Ca(OH)_2$ treated natural clinoptilolite. Chem Eng J 320:510–522. https://doi.org/10.1016/j.cej.2017.03.063

Sarkar A, Biswas SK, Pramanik P (2010) Design of a new nanostructure comprising mesoporous ZrO_2 shell and magnetite core (Fe_3O_4@mZrO_2) and study of its phosphate ion separation efficiency. J Mater Chem 20(21):4417–4424. https://doi.org/10.1039/b925379c

Seviour RJ, Mino T, Onuki M (2003) The microbiology of biological phosphorus removal in activated sludge systems. FEMS Microbiol Rev 27(1):99–127. https://doi.org/10.1016/S0168-6445(03)00021-4

Wang W et al (2015) Adsorptive removal of phosphate by magnetic Fe_3O_4@C@ZrO_2. Colloids Surf, A 469:100–106. https://doi.org/10.1016/j.colsurfa.2015.01.002

Weber W (1963) Kinetics of adsorption on carbon from solution. J Sanit Eng Div 89(2):31–59

Worsfold P, McKelvie I, Monbet P (2016) Determination of phosphorus in natural waters: a historical review. Anal Chim Acta 918:8–20. https://doi.org/10.1016/j.aca.2016.02.047

Wu R et al (2014) Hydrothermal preparation of magnetic Fe_3O_4@C nanoparticles for dye adsorption. J Environ Chem Eng 2(2):907–913. https://doi.org/10.1016/j.jece.2014.02.005

Wu B et al (2017a) Highly efficient and selective phosphate removal from wastewater by magnetically recoverable $La(O.H.)_3/Fe_3O_4$ nanocomposites. Water Res 126:179–188. https://doi.org/10.1016/j.watres.2017.09.034

Wu Z, Gao D, Liu N (2017b) Adsorption behavior of phosphate on anion-functionalized nanoporous polymer. Water Qual Res J Can 52(3):187–195. https://doi.org/10.2166/wqrj.2017.008

Xuan S et al (2007) A facile method to fabricate carbon-encapsulated Fe_3O_4 core/shell composites. Nanotechnology. https://doi.org/10.1088/0957-4484/18/3/035602

Yang J et al (2011) A designed nanoporous material for phosphate removal with high efficiency. J Mater Chem 21(8):2489–2494. https://doi.org/10.1039/c0jm02718a

Zhang J et al (2010) Adsorption behavior of phosphate on Lanthanum (III) doped mesoporous silicates material. J Environ Sci 22(4):507–511. https://doi.org/10.1016/S1001-0742(09)60141-8